NASA Technical Memorandum 106752
ICOMP–94–24

The Flow Induced by the Coalescence of Two Initially Stationary Drops

M.R. Nobari
University of Michigan
Ann Arbor, Michigan

and

G. Tryggvason
Institute for Computational Mechanics in Propulsion
Lewis Research Center
Cleveland, Ohio

and University of Michigan
Ann Arbor, Michigan

October 1994

National Aeronautics and
Space Administration

THE FLOW INDUCED BY THE COALESCENCE OF TWO INITIALLY STATIONARY DROPS

M.R. Nobari
The University of Michigan
Department of Mechanical Engineering
Ann Arbor, MI 48109

G. Tryggvason
Institute for Computational Mechanics in Propulsion
Lewis Research Center
Cleveland, OH 44135
and
The University of Michigan
Department of Mechanical Engineering
Ann Arbor, MI 48109

ABSTRACT

The coalescence of two, initially stationary drops of different size is investigated by solving the unsteady, axisymmetric Navier-Stokes equations numerically, using a Front-Tracking/Finite Difference method. Initially, the drops are put next to each other and the film between them ruptured. Due to surface tension forces, the drops coalesce rapidly and the fluid from the small drop is injected into the larger one. For low nondimensional viscosity, or Ohnesorge number, little mixing takes place and the small drop fluid forms a blob near the point where the drops touched initially. For low Ohnesorge number, on the other hand, the small drop forms a jet that penetrates far into the large drop. The penetration depth also depends on the size ratio of the drops and we show that for a given fluid of sufficiently low viscosity, there is a maximum penetration depth for intermediate size ratios.

I. INTRODUCTION

The motivation for the present work is an experiment presented recently by Anilkumar, Lee, and Wang (1991). In their study, two drops of the same fluid, but of unequal size, were slowly brought together until the film between them ruptured and the drops coalesced. The fluid motion following the rupture was recorded on a video tape, and by coloring the fluid in the small drop the resulting flow could be observed. For high viscosity drops the fluid from the smaller drop simply became a flat blob inside the large drop near the point of initial contact, but for low viscosity drops the fluids mixed considerably. This was due to the formation of a jet of the fluid from the small drop, that was injected into the large drop by the action of surface tension. Anilkumar *et al* did not investigate the mixing of the two drops in any detail, turning their attention instead to the coalescence of a single drop with a flat interface. Here, we extend the study of Anilkumar *et al* by simulating numerically the fluid motion in the drops following the rupture of the film between them.

The post-rupture behavior of drops of different size, in particular the flow within the drops, appears to have received relatively little attention. Apart from the report by Anilkumar *et al*, we have only found a brief description in a paper by MacKay and Mason (1963), who were primarily interested in the time of rupture and whether the coalescence lead to a secondary drop. They therefore did not address the mixing of the fluids at all. Two related problems have, however, been extensively examined; the coalescence of equal size drops, and the coalescence of drops with a free surface or a fluid interface. These investigations can be further divided into collisions where the drops approach each other (or a fluid interface) with a finite velocity and the case where the drops are brought together sufficiently slowly so that the initial kinetic energy is negligible. For the problem of interest here, the latter case is of most relevance. For a discussion of the former, see Nobari, Jan, and Tryggvason (1993) and Azhgriz and Poo (1990) for the collision of two drops, and Rein (1993) for the collision of a drop with a free surface.

The focus of research on the coalescence of equal size drops, brought in contact slowly, has been mainly on the draining of the film between the drops and the time of rupture of this film. Experimental measurements (MacKay and Mason, 1963, for example) predict that this spontaneous rupture of the film occurs when the film thickness is about $0.05\mu m$. Recent work on this problem, as well as several references, can be found in Yiantsos and Davis (1991) and Jacqmin and Foster (1993), for example.

The generation of vortex rings by drops colliding with a flat interface has been studied by a number of authors. One of the earliest such investigations is due to Thomson and Newall (1885) who found that drops falling into a pool of liquid form vortex rings only at small impact velocities. Higher velocities lead to a splash and a relatively small penetration depth of the drop fluid. The question of how rapidly small drops fall to a flat interface and coalesce with it is of relevance to the stability of emulsions, and a number of investigations in the fifties and sixties examined the problem in that context. Here, a drop approaches an interface with nearly zero velocity and the main question is how fast the film of fluid between the drop and the interface drains and ruptures. Examples of these studies can be found in Gillesepie and Rideal (1956) and Nielson et al. (1958), and Charles and Mason (1960), for example. The last authors found that in some cases the coalescence is completed in several stages, where a part of the initial drop coalesces and the rest generates a secondary drop. This process continues until the remaining drop coalesces without forming a secondary drop. None of these authors appears to have considered the subsequent mixing of the liquids. An example of a more recent study can be found in Chapman and Critchlow (1967) who investigated the formation of vortex rings from falling drops, and concluded that the shape of the drop at the moment of contact has great effect on the formation of the vortex ring. This was investigated further by Rodriguez and Mesler (1988) who also found that the shape had considerable influence on the vortex ring formation, but gave a different explanation than Chapman and Critchlow. The boundaries between the regimes where drops colliding with an interface form a vortex ring and where they splash has been investigated by Rodriguez

and Mesler (1985) and Hsiao, Lichter, and Quintero (1988), for example. Anilkumar *et al* (1991) examined drops that approach an interface with essentially zero velocity and developed a corrilation for the penetration depth. For a recent review of the litterature on drops colliding with a liquid surface, including a detailed discussion of when drops splash and when they form a vortex ring, see Rein (1993).

In this paper we focus on the fluid mixing due to the coalescence of a large and a small drop. We simulate the motion of several pairs and examined how far the fluid from the small drop penetrates the larger one, as a function of the size ratio of the drops and the nondimensional viscosity. In section II we formulate the problem and describe our numerical method briefly. Results and discussions are in section III, and section IV contains our conclusions.

II. FORMULATION and NUMERICAL METHOD

The coalescence of two drops is a complicated process where it is necessary to account for several physical processes simultaneously. The drops are driven together by surface tension; inertia and viscosity determine the resulting mixing of the fluids; and surface tension and inertia govern the resulting oscillations. The solution of this problem therefore requires the full Navier-Stokes equations.

The momentum equations, considering the motion of both the drop and the ambient fluid, allowing discontinuous viscosity and density, and including surface tension forces, can be expressed as one set of equations. For axisymmetric flows these are:

$$\frac{\partial \rho v_r}{\partial t} + \frac{1}{r}\frac{\partial}{\partial r} r \rho v_r^2 + \frac{\partial}{\partial z}\rho v_z v_r = -\frac{\partial p}{\partial r} + \frac{\partial}{\partial r} 2\mu \frac{\partial v_r}{\partial r} + 2\mu \frac{\partial}{\partial r}\left(\frac{v_r}{r}\right) + \frac{\partial}{\partial z}\mu\left(\frac{\partial v_z}{\partial r} + \frac{\partial v_r}{\partial z}\right) + F_r \tag{1}$$

$$\frac{\partial \rho v_z}{\partial t} + \frac{1}{r}\frac{\partial}{\partial r} r \rho v_r v_z + \frac{\partial}{\partial z}\rho v_z^2 = -\frac{\partial p}{\partial z} + \frac{1}{r}\frac{\partial}{\partial r}\mu r\left(\frac{\partial v_z}{\partial r} + \frac{\partial v_r}{\partial z}\right) + \frac{\partial}{\partial z} 2\mu \frac{\partial v_z}{\partial z} + F_z \tag{2}$$

Here, z and r are the axial and the radial coordinate, respectively, and v_z and v_r the corresponding velocity components. p is the pressure, and ρ and μ are the discontinuous density and viscosity fields, respectively. $\mathbf{F} = (F_r, F_z)$ is the surface tension force and only acts where the fluid interface is. $\mathbf{F}$ can be written in the following form:

$$\mathbf{F} = \int_F \frac{1}{r}\Big(\frac{\partial}{\partial s}(r\sigma\mathbf{t}) - \sigma\mathbf{i}_r\Big)\delta_{rz}(\mathbf{x} - \mathbf{x}_f)ds \tag{3}$$

where $\mathbf{i}_r$ is a unit vector in the r-direction, $\mathbf{t}$ is a tangent vector to the drop surface in the (r, z) plane, δ_{rz} is a two-dimensional delta function and $\mathbf{x} = (r, z)$. $\mathbf{x}_F$ is the position of the interface.

The above equations are supplemented by the incompressiblity condition

$$\frac{1}{r}\frac{\partial}{\partial r}rv_r + \frac{\partial}{\partial z}v_z = 0 \tag{4}$$

which, when combined with the momentum equations leads to a non-separable elliptic equation for the pressure. We also need equations of state for the density and viscosity, which in our case are:

$$\frac{D\rho}{Dt} = 0; \qquad \frac{D\mu}{Dt} = 0. \tag{5}$$

These equations simply state that density and viscosity within each fluid remains constant at all times.

The nondimensional parameters describing the coalescence of two drops of different size are the size ratio of the drops and the Ohnesorge number, which can be interpreted as a nondimensional viscosity:

$$\lambda = d_s/D; \qquad Oh = \frac{\mu_d}{\sqrt{\sigma\rho_d d_s}} \tag{6}$$

Here, μ_d is the viscosity of the drops, d is the drop diameter, and $D = (d_l^3 + d_s^3)^{1/3}$ is the diameter of the drop that results after the small and the large drop have coalesced. The subscripts s and l refer to the small and the large drop, respectively. Obviously, we could have selected either d_l or D for Oh, but as the subsequent discussion will show, d_s is the most natural choice. To completely specify the problem, the density ratio, ρ_o/ρ_d, and the viscosity ratio, μ_o/μ_d, must also be given.

After the drops coalesce, the combined drop oscillates. The period of oscillations, τ_D, plays a major role in determining the time scale of the motion and we will compare our results with Lamb's (1932) formula:

$$\tau_n = \frac{\pi}{\sqrt{n(n-1)(n+2)}}\sqrt{\frac{\rho d^3}{2\sigma}} \tag{7}$$

Here, n is the order of the mode and the lowest oscillatory mode has $n = 2$. Other authors have extended this formula to include the density of the outer fluid and discussed the effects of nonlinearities and viscosity. In our case these corrections have only secondary influence. When we present our results, time is given in units of $\tau_D = \tau_{n=2}$.

For low viscosity, the oscillations of the resulting drop are reduced slowly and it would require a long time to compute the evolution until the final stationary state. Since a relatively fine grid is necessary, such computations would be excessively demanding on our computational resources. To shorten the computations we set the viscosity of the ambient fluid higher than the viscosity of the drop fluid. This leads to a high damping of the drop oscillations, but has little effect on the mixing process. In some experimental studies of drop coalescence, a high viscosity host fluid has been used to allow the drops to be brought in contact slowly (Anilkumar *et al.*, 1991).

To solve the Navier-Stokes equations numerically, we use a finite difference/front tracking method developed by Unverdi and Tryggvason (1991a,b). The actual code is an axisymmetric version of the method written by Y.-J. Jan (Jan, 1994). The method is based on solving a single set of equations (equations 1 and 2) for the whole computational domain, both inside and outside the drops. By adding the surface tension force by a delta function the correct stress boundary conditions are implicitly enforced. We use a regular, fixed, staggered mesh; a second order, centered difference approximation for all spatial derivatives, and a simple explicit, first order method for the time discretization. We have also used a second order time integration for other problems and generally find little differences for short times as those simulated here. Instead of solving equations (5) to update the density and viscosity field directly,

we introduce a line of connected marker particles, or a front, that moves with the fluid and marks the boundary of the drops. At every time step the density and the viscosity field are updated using the new position of the front by a technique described in Unverdi and Tryggvason (1991). The front is also used to compute the surface tension forces, which are then assigned to the grid points next to the front and used to compute the new velocity field. Both the method and the code have been extensively validated by comparison with linear solutions, by comparison with other numerical studies (Ryskin and Leal, 1984, for example), and by examining the rate of convergence under grid refinement. For a discussion of some of these tests, as well as other applications of the method see, for example: Unverdi and Tryggvason (1991a,b) who simulated the rise of buoyant bubbles and the three-dimensional collision of two bubbles; Jan and Tryggvason (1993) who examined the effect of contaminant on the rise of axisymmetric bubbles; Nobari, Jan and Tryggvason (1993) and Nobari and Tryggvason (1993) who simulated the collision of axisymmetric and three-dimensional drops; and Nas and Tryggvason (1993) who computed the thermal migration of many bubbles. The computations presented here were done on an HP735 workstation. The time required for each runs depended on Oh, but was about three days for the highest Oh used.

III. RESULTS and DISCUSSION

Figure 1 shows a sketch of the computational setup. The domain is an axisymmetric cylinder of length three times its radius and the diameter of the large drop is half the diameter of the cylinder. The domain is resolved by a regular, staggered mesh, and for the computations presented here we have used a 100 by 300 grid. Several of the computations have also been repeated on coarser grids. For the lower values of Oh little differences are observed, but for the highest values of Oh, small oscillations appear near the centerline at lower resolution. The rest of the solution is minimally affected. The density of the drops is twenty times the density of the ambient fluid in all the computations presented here, and the viscosity ratio, the Ohnesorge number,

and the size ratio are listed in the figure caption. Initially, the drops are placed next to each other with the centers of the drops two percent closer than half the sum of the radii. The surfaces that overlap are removed to form a small opening, or a connecting hole, between the drops. Thus, we completely side step the question of when the film between the drop ruptures. We have examined the effect of the size of this opening and found that once it is sufficiently small, as it is here, the resulting motion is independent of its size. Once it becomes larger, however, the initial surface tension energy is reduced and this causes less penetration of the fluid from the small drop. Since the drops are initially spherical, the contact area is relatively small and while it is possible that small drops are generated during the initial enlargement of the original rupture, (as discussed by Oguz and Prosperetti, 1990, for example) we assume that those are sufficiently small so that they do not affect the rest of the evolution. We also assume that any non-axisymmetric aspect of the actual rupturing quickly dissappear as the neck is pulled outward. This is in line with the observations of Anilkumar *et al.*

Figure 2 and 3 show the coalescence of two drops, where the small drop diameter is half the diameter of the large drop, for two values of Oh. In figure 2, $Oh = 0.0162$ and in figure 3, $Oh = 0.0024$. Although the computations are axisymmetric, the figures are given a fully three-dimensional appearance by rotating the surfaces around the symmetry axis. The large drop is transparent but the small drop is not. In both cases, the small drop is rapidly pulled into the large drop, causing it to oscillate. Since the outer fluid has a high viscosity, these oscillations die out rather quickly. The major difference between the two simulations is the viscosity of the drop fluid. In figure 2 it is high and the small drop eventually forms a stationary blob at the point where the drops touch initially. In figure 3, on the other hand, the viscosity is low and the fluid from the small drop forms a jet that penetrates to the other side of the large drop. This evolution is quantified in figure 4 where the distance between the poles of the combined drop and the length of the blob of fluid from the small drop are plotted versus time. The results for the run in figure 2 is shown in (a), and (b)

corresponds to figure 3. Similarly, figure 5 shows the energies, non-dimensionalized by the combined initial surface tension energy of both drops, for both cases. The left column corresponds to figure 2 and the right column to figure 3. In the top row, the surface energy, kinetic energy and the total energy for the combined drop is plotted versus time and in the bottom row the kinetic energy of the fluid from the small drop is plotted separately, along with the total kinetic energy.

The results in figures 2-5 provide a detailed picture of the coalescence process: The initial coalescing of the drops takes place in two stages. First, the "waist" where the drops touch, is pulled outward due to the high curvature around the initial hole. Fluid to fill this space is drawn from both the small and the large drop, leading to considerable reduction in the diameter of the small drop. Once this initial motion is completed (second frame in figures 2 and 3) the small drop is pulled into the large drop extremely rapidly. This "pull-in" is shown by the rapid shortening of the maximum distance between the poles of the combined drop in figure 4, and the small drop has been completely engulfed into the large drop at about t=0.3 for both the low and the high viscosity case. The time it takes for the large drop to swallow the little one is thus very close to the period of oscillation for the lowest order mode of the small drop. In the units used here—the periode of oscillation of the final drop—this periode is 0.33. The injection of the small drop is accompanied by a rapid decrease of surface tension energy (figure 5). At the same time, the kinetic energy of the small drop (figure 5-bottom row) increases rapidly, peaks, and then decreases equally rapidly. Notice that the rate of dissipation of total energy is increased sharply as the kinetic energy of the small drop increases, but that its decay rate falls back to normal after the maximum is reached, indicating that some of the loss of the kinetic energy from the small drop goes to increase the kinetic energy of the fluid in the large drop. Since the outer fluid has a larger viscosity, the oscillations of the resulting drop are damped quickly.

This relatively complex initial motion is nearly identical for both the high and the low viscosity case. Indeed, the only difference is the higher kinetic (and therefore

total) energy for the low viscosity simulation. Following the initial injection, the motion of the fluid from the small drop depends strongly on the viscosity. In figure 2, where the viscosity is high, its kinetic energy is quickly dissipated and the fluid from the small drop simply remains where it was injected. For the low viscosity fluid, on the other hand, the vorticity injected during the engulfment of the small drop drives the blob into the large drop, forming a jet with a vortex ring at its tip. The vorticity eventually diffuses and at the end of the run the fluid from the small drop simply moves with the large drop as it oscillates. While the mixing in these two cases is very different, the oscillations of the resulting drop are similar. The motion of the more viscous drops falls off slightly faster, but overall the damping of the oscillations seems to be mostly due to the high viscosity of the outer fluid. The period of the final large scale oscillations is nearly equal to $\tau_{n=2}$, but initially, higher modes are also seen. The shape of the drop in figures 2 and 3 suggests that the $n = 3$ mode (with two times the frequency of the fundamental mode) is excited by the initial conditions, and the graphs in figure 4 and 5 indicate the presence of even higher modes. All but the lowest order modes are quickly damped.

The flow induced by the low viscosity jet in figure 3 is shown in figure 6, where the streamlines for both the drop and the ambient fluid is shown at two times. In the first frame, at t=1.25, the bottom and the top of the drop are moving downward; the lower side of the drop is moving inward and the upper side outward, thus characteristic of a $n = 3$ oscillation. Near the tip of the jet, the streamlines form a closed loop, enclosing the vorticity there. In the other frame, at t=2.5, the jet has nearly reached the top of the drop. The boundary of the fluid from the small drop has rolled up to form a vortex ring and the circular streamlines show that there is still some vorticity present near the tip of the jet. The flow field has also changed. The top of the drop is now moving down and the bottom is moving up as the middle of the drop moves outward, due to a $n = 2$ oscillation. Notice, that as the jet moves into the drop, there is a small backflow near the base of the jet and a small striation of the outer fluid is entrained into the jet.

The evolution of drops of a different size ratio ($d_s/D = 0.667$) is shown in figure 7, where the surface of the drops and the boundary between the fluids from the large and the small drop are shown at selected times. The viscosity of the drops is relatively low here, $Oh = 0.002$, so if the ratio of the diameters was the same as in the previous computations we would expect a jet that penetrated all the way across the large drop. While the overall evolution is similar to figure 3, there are noticeable differences. The initial engulfment of the small drop causes large deformation of the large drop, and although a jet is formed, it does not form a vortex ring and does not penetrate all the way across the large drop. The entrainment of fluid from the large drop near the base of the jet is stronger and this striation rolls up, indicating the presence of vorticity within the blob of fluid from the small drop. Figure 8a shows the distance between the top and bottom of both the combined drop and the fluid from the small drop (as in figure 4), and figure 8b shows the surface tension, kinetic, and total energy for the combined drop (as in figure 5-top row). The major difference between the evolution here and the runs in figures 2 and 3, where the size difference is larger, is that the oscillations of the drop are both larger in amplitude and contain less of the higher order modes. Obviously, if the drops were of exactly equal size, only the even modes would be excited and while the drops are not of the same size, they are sufficiently close so that this is still the case.

The quantity that is most easily observed experimentally is the eventual penetration depth of the fluid from the small drop, L. For a given Oh, two limits are easily determined. As the small drop becomes very small, viscosity must eventually dominate the evolution so $L/D \to 0$ as $d_S/D \to 0$. In the other limit, the drops are of equal size and since there is no penetration, by symmetry, we must have $L/D \to 1/2$ as $d_S/D \to \sqrt[3]{\frac{1}{2}} = 0.794$. For small drops, we expect the size of the large drop to have little influence on the evolution and the results of a drop coalescing with a flat interface should apply. Anilkumar *et al* (1991) found that the penetration depth was well described by

$$\frac{L}{d_S} = \frac{K}{\sqrt{Oh}} \tag{7}$$

where $K = 0.68$ yielded a best fit to their experimental results. Rewriting this in our variables gives

$$\frac{L}{D} = \frac{K}{\sqrt{Oh}} \frac{d_S}{D} \tag{10}$$

so the penetration depth goes to zero linearly with a slope that depends on Oh for small drops. The simplicity of this expression is the main reason for using d_s in Oh—any other choice would have lead to a more complex dependency on the size ratio. Figure 9 shows the numerically computed penetration depth, L/D, versus the ratio of the small drop diameter to the diameter of the combined drop, d_S/D, for several values of Oh. We have not computed the evolution for very small drops since this would require very fine resolution, but we do include the limit predicted by the experiments of Anilkumar *et al* (1991) as solid lines to the left of the graph, near the origin. We note that for a given Oh, the penetration depth has a maximum for intermediate d_S/D. In more physical terms, this means that the penetration depth is largest when the small drop is neither very small nor comparable in size to the large drop. This conclusion is obviously only valid for drops of relatively small viscosity (small Oh). For very viscous drops the penetration depth varies monotonically from zero for small d_S/D to a half for drops of equal size. The shaded region at the bottom of the graph is the minimum penetration depth, obtained by assuming that the surface separating the fluids in the final drop is flat. The dashed line is an extrapolation from our data and the correlation of Anilkumar *et al* for Oh=0.0024.

Although we expect the computations presented here to give a fairly complete picture of the evolution in the range of size ratios and Oh simulated, we are—as always in computational investigations—limited by the available resolution to situations where the ratio of the largest to the smallest scale is not too large. Here, this prevents us from going to very low Oh and d_S/D. While there is no reason to believe that any new phenomena will be observed at large d_S/D (drops of similar size) by lowering the Oh further, two aspects of the evolution for small d_S/D are outside the range of parameters that we have simulated. For very large ratio of the drop diameters (small d_S/D), it is possible for the drops to undergo partial coalescence (if the viscosity of

the drop and the ambient fluid are similar) where only a part of the small drop is engulfed into the large one, leaving a small secondary drop. This was seen by MacKay and Mason (1963) for a drop coalescing with a flat interface. The second possible new phenomena is if the jet penetrates through the large drop and forms another drop on the other side. The formation of drops by a vortex ring colliding with a flat interface has been investigated by Bernal, Maksimovic, Tounsi, and Tryggvason (1994) and based on those results we would only expect this to happen at very low Oh and small d_S/D. Even if the jet reaches the other side of the drop and forms a "bulge" there, it is likely that in most cases this "bulge" would be pulled back into the large drop and that $L/D = 1$ is a practical upper bound for the penetration depth.

IV. CONCLUSIONS

We have computed the coalescence and mixing of two drops for different size ratios and different values of the nondimensional viscosity, Oh. The computations show that the fluid from the small drop forms a jet that can penetrate far into the large drop for intermediate size ratios and low dissipation. This jet can lead to a relatively large mixing between the fluids from the small and the large drop. For larger dissipation the fluid from the small drop forms a "blob" near the original injection point and little or no mixing takes place. For drops of nearly equal size, little mixing takes place and for very small drops, viscosity dissipates the jet quickly. We have only computed the evolution for a relatively few cases and while these results do not provide the function $L/D = f(\lambda, Oh)$ in detail, the general shape is clear. The results agree well with the experimental results of Anilkumar *et al* (1991), but detailed quantitative comparison is not possible since little data was reported by them.

The results here show well the fundamental role the frequency of oscillations of the lowest mode plays for droplet motion. The initial coalescence process is well predicted by the period of the small drop and while higher order modes are triggered initially, the resulting drop eventually oscillates with its fundamental frequency. We note that similar dependency is found for bouncing collision of drops where the collision time is

nearly equal to the period of the lowest oscillatory mode, even when large deformation occurs.

The dynamics of the coalescence and the subsequent mixing process depends on viscosity, inertia and surface tension, and accurate simulation of the process requires solutions of the full Navier-Stokes equations. As such, this problem is an excellent test case for the method used here and the results suggest that the technique is well capable of resolving all the important physical processes.

ACKNOWLEDGMENT

We would like to thank Y.-J. Jan for allowing us to use his numerical code, and to acknowledge discussions with Dr. D. Jacqmin at the NASA Lewis Research Center. This work was supported by NASA grant NAG3-1317. Part of this work was done while one of the authors (GT) was visiting the Institute for Computational Mechanics in Propulsion at NASA Lewis. Some of the computations were done at the San Diego Supercomputing Center which is funded by the National Science Foundation.

REFERENCES

A.V. Anilkumar, C.P. Lee, and T.G. Wang. Surface-Tension-Induced Mixing Following Coalescence of Initially Stationary Drops. Phys. Fluids A. **3** (1991), 2587-2591.

N. Azhgriz and J.Y. Poo. Coalescence and Separation in Binary Collisions of Liquid Drops. J. Fluid Mech. **221** (1990), 183-.

L.P. Bernal, P. Maksimovic, F. Tounsi, and G. Tryggvason. An Experimental and Numerical Investigation of Drop Formation by Vortical Flows in Microgravity. AIAA 94-0244

D.S. Chapman and P.R. Critchlow. Formation of Vortex Rings from Falling Drops. J. Fluid Mech. **29** (1967), 177-185.

G.E. Charles and S.G. Mason. The Mechanism of Partial Coalescence of Liquid Drops at Liquid/Liquid Interfaces. J. Colloid Sci. **15** (1960), 105-122.

T. Gillespie and E.K. Rideal. The Coalescence of Drops at an Oil-Water Interface. Trans. Faraday Soc. **52** (1956), 173-183.

M. Hsiao, S. Lichter, and L.G. Quintero. The Critical Weber Number for Vortex and Jet Formation for Drops Impinging on a Liquid Pool. Phys. Fluids **31** (1988) 3560-3562.

D. Jacqmin and M.R. Foster. The Evolution of Thin Films Generated by the Collision of Highly Deforming Droplets. Submitted for publication (1993).

Y.J. Jan and G. Tryggvason. The Rise of Contaminated Bubbles. Submitted for publication.

Y.-J. Jan. Ph.D. Thesis, Computational Studies of Bubble Dynamics. The University of Michigan, 1994.

H. Lamb. Hydrodynamics. Dover Publishers, New York, (1932), 738 pages.

G.D.M. MacKay and S.G. Mason. The Gravity Approach and Coalescence of Fluid Drops at Liquid Interfaces. Can. J. Chem. Eng. **41** (1963), 203-212.

S. Nas and G. Tryggvason. Computational Investigation of the Thermal Migration of Bubbles and Drops. In AMD 174/FED 175 Fluid Mechanics Phenomena in Microgravity, Ed. Siginer, D. A., Thompson, R. L. and Trefethen, L. M. 1993 ASME Winter Annual Meeting. Pages 71-83

L.E. Nielsen, R. Wall, and G. Adams. Coalescence of Liquid Drops at Oil-Water Interfaces. J. Colloid Sci. **13** (1958), 441-458.

M.R. Nobari, Y.-J. Jan, and G. Tryggvason. Head-On Collision of Drops—A numerical Investigation. Submitted for publication.

M.R. Nobari and G. Trygvason. Numerical Simulation of Drop Collisions. AIAA paper 94-0835.

H.N. Oguz and A. Prosperetti. Bubble entrainment by the impact of drops on liquid surfaces. J. Fluid Mech. **219** (1990), 143-179.

M. Rein. Phenomena of liquid drop impact on solid and liquid surfaces. Fluid Dyn.

Res. **12** (1993), 61-93.

F. Rodriguez and R. Mesler. Some drops don't splash. J. Colloid. Interface Sci. **106** (1985), 347-352.

F. Rodriguez and R. Mesler. The Penetration of Drop-Formed Vortex Rings into Pools of Liquid. J. Colloid Sci. **121** (1988), 121-129.

G. Ryskin and L.G. Leal. Numerical solution of free-boundary problems in fluid mechanics. Part 2. Buoyancy-driven motion of a gas bubble through a quiescent liquid. J. Fluid Mech. **148** (1984), 19-35.

J.J. Thomson, H.F. Newall. On the Formation of Vortex Rings by Drops Falling into Liquids, and some Allied Phenomena. Proc. London Math. Soc. (1885), 417-436.

S.O. Unverdi and G. Tryggvason. A Front Tracking Method for Viscous Incompressible Flows. J. Comput. Phys., **100** (1992) 25-37.

S.O. Unverdi and G. Tryggvason. Multifluid Flows. Physica D **60** (1992) 70-83.

S. Yiantsios and R. Davis. Close Approach and Deformation of Two Viscous Drops Due to Gravity and Van der Waals Forces. J. Coll. Interface Sci. **144** (1991), 412-433.

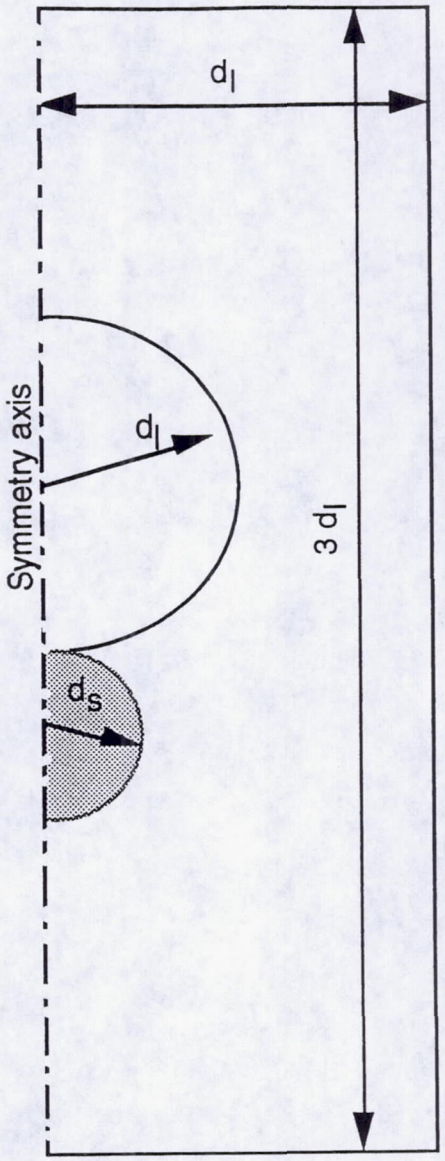

Figure 1. A sketch of the computational setup. The domain is an axisymmetric cylinder of length three times its diameter. The diameter of the large drop is half the diameter of the cylinder.

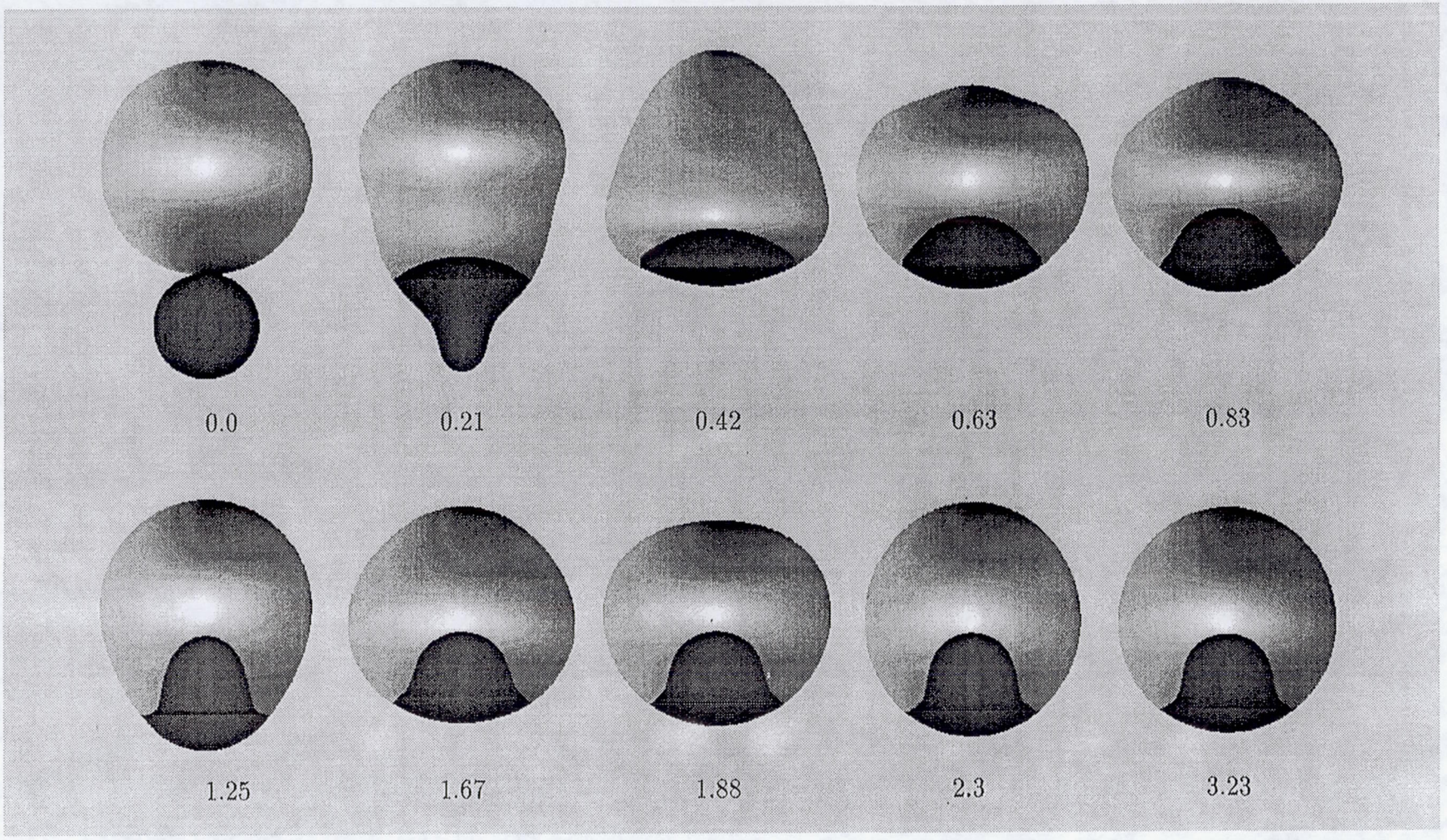

Figure 2. The evolution of two drops of unequal size following coalescence. Here, the viscosity of the drops is high, $Oh = 0.0162$, and the fluid from the small drop remains near the initial point of contact. $d_s/D = 0.481$, $\rho_d/\rho_o = 20.0$, and $\mu_d/\mu_o = 0.667$.

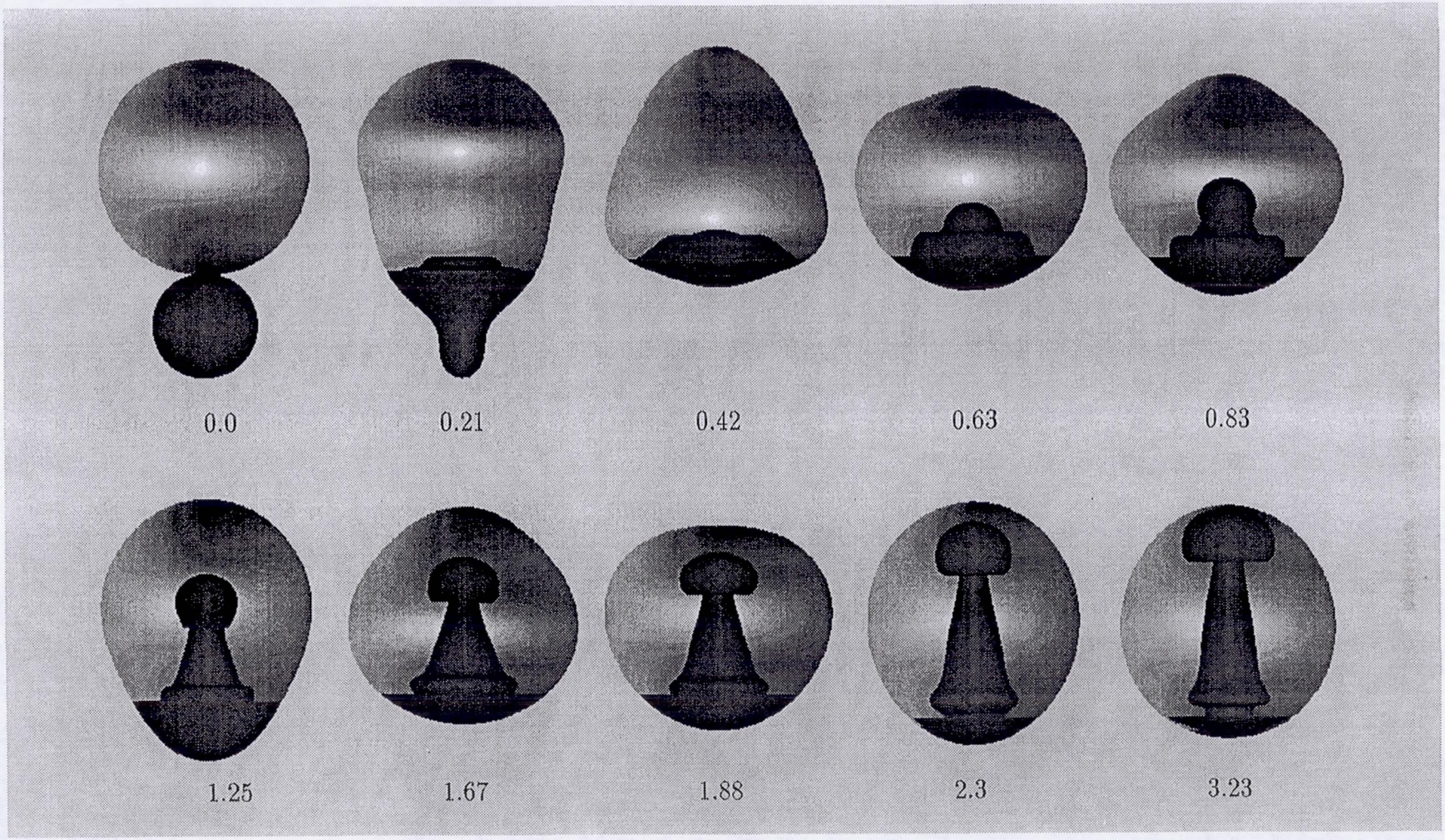

Figure 3. The evolution of two drops of unequal size following coalescence. Here, the viscosity of drops is low, $Oh = 0.0024$, and the fluid from the small drop penetrates across the large drop. $d_s/D = 0.481$, $\rho_d/\rho_o = 20.0$, and $\mu_d/\mu_o = 0.1$.

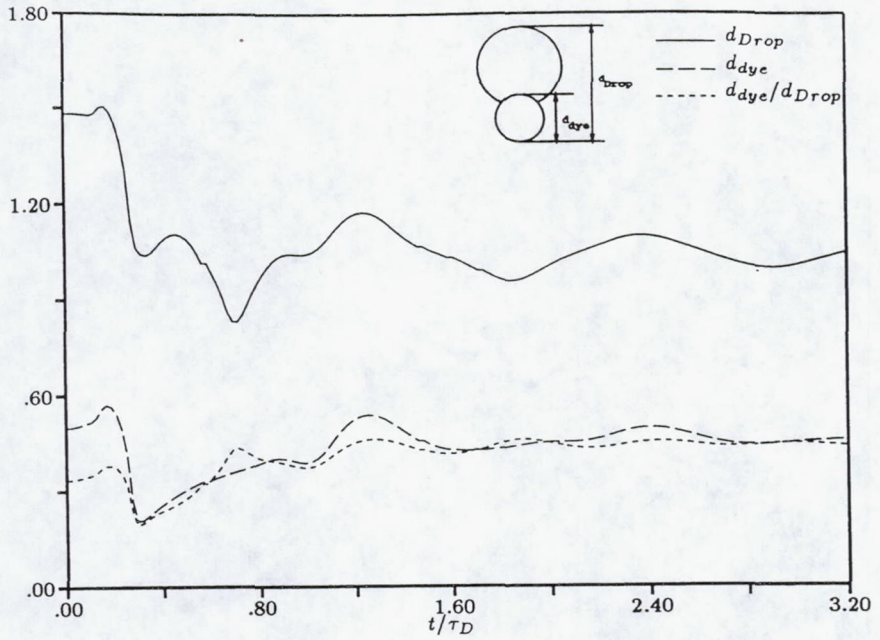

(a)

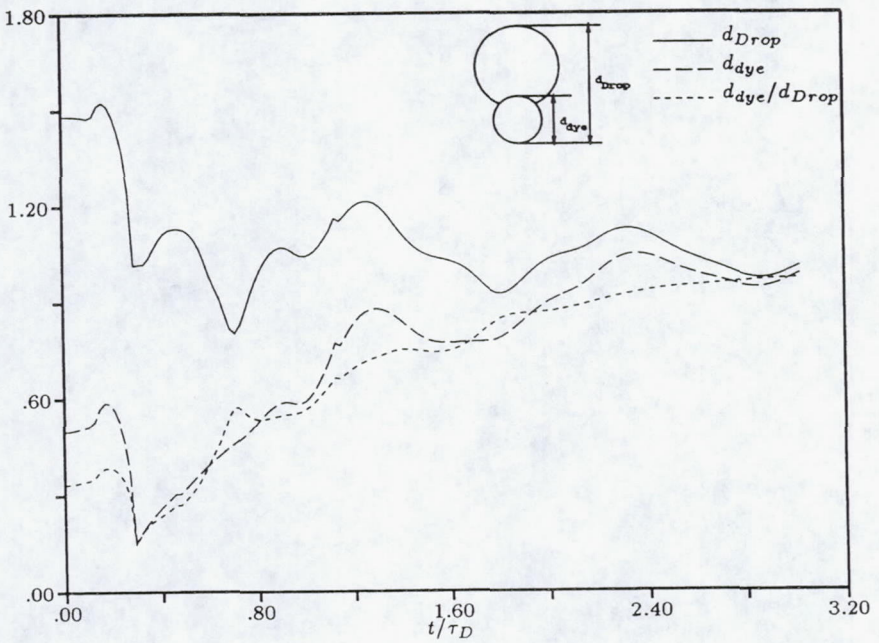

(b)

Figure 4. Axial distance, penetration depth, and their ratio, versus time. $Oh = 0.0162$ in (a) and $Oh = 0.0024$ in (b). Non-dimensional time is based on τ_D, the fundamental period of oscillation of the coalesced drop.

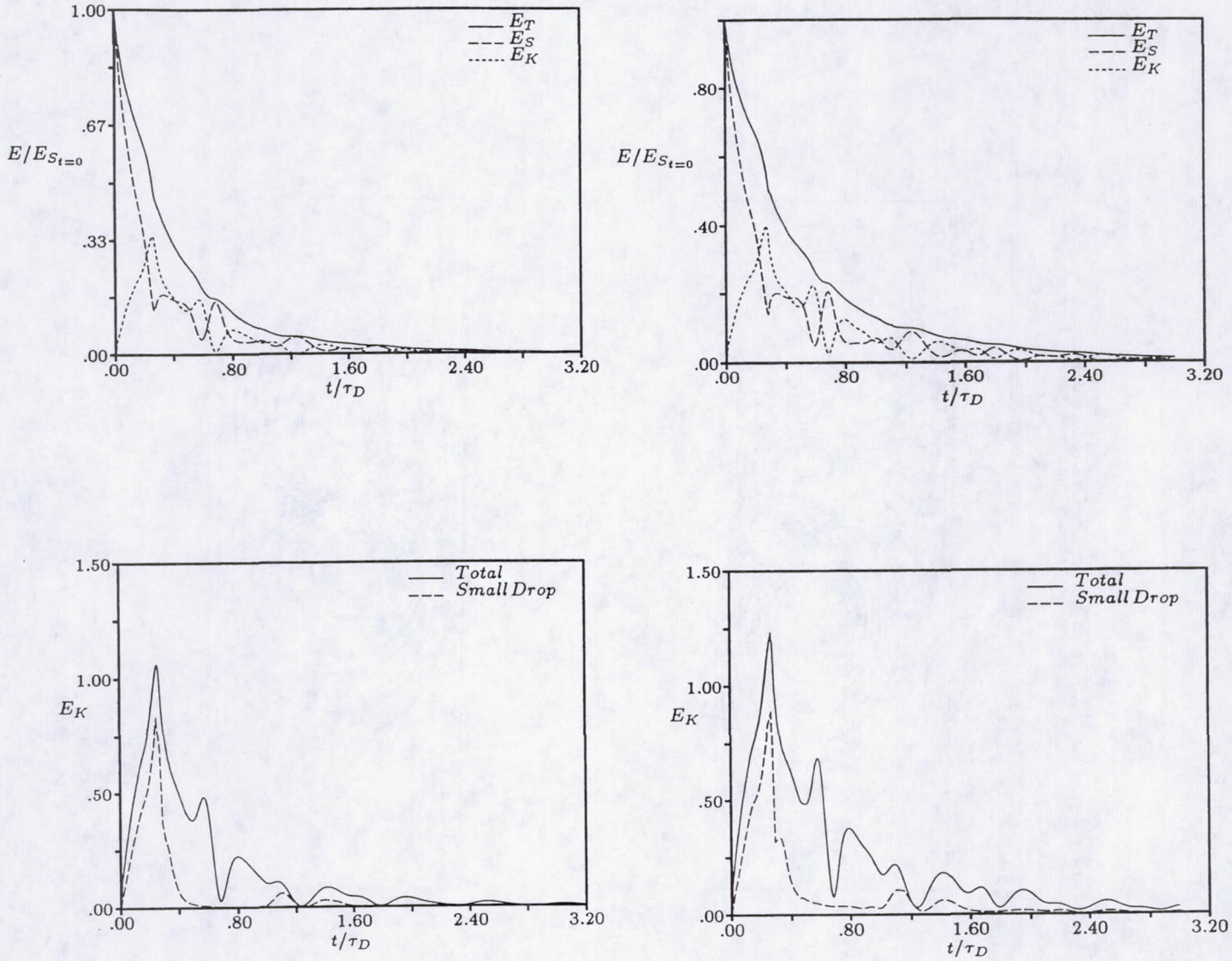

Figure 5. Top row: Non-dimensional kinetic, surface tension, and total energy versus time for the drops in figures 2 and 3. Bottom row: Total kinetic energy and the kinetic energy of the small drop versus time. Left column: $Oh = 0.0162$. Right Column: $Oh = 0.0024$.

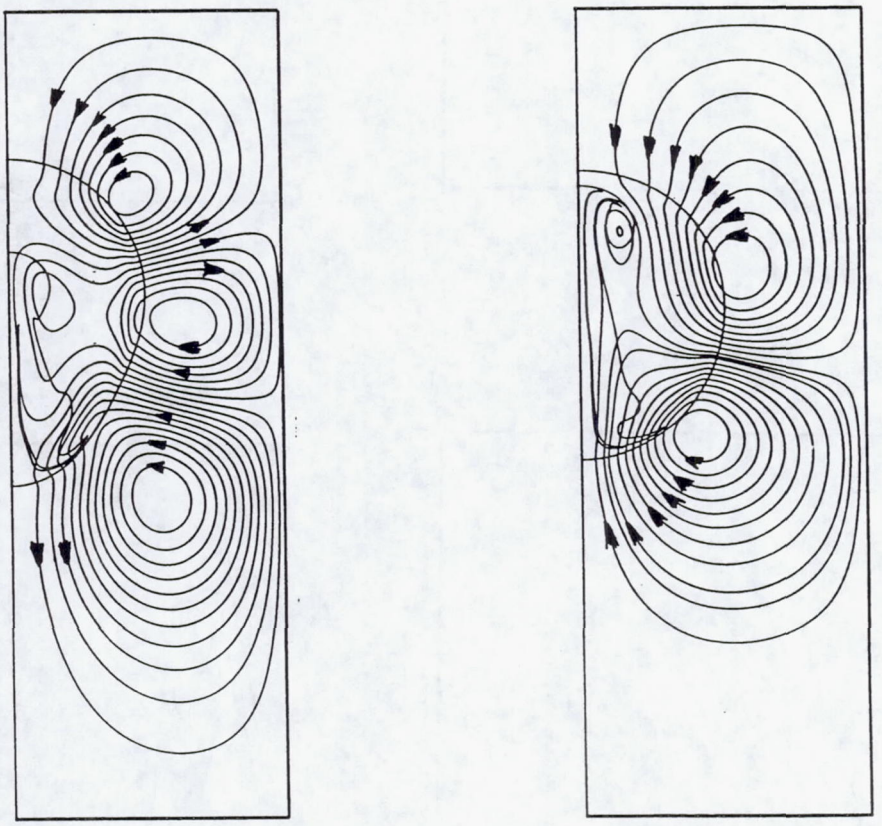

Figure 6. The streamlines for the low viscosity drops in figure 3 at times $t/\tau_D = 1.25$ (left) and $t/\tau_D = 2.5$ (right).

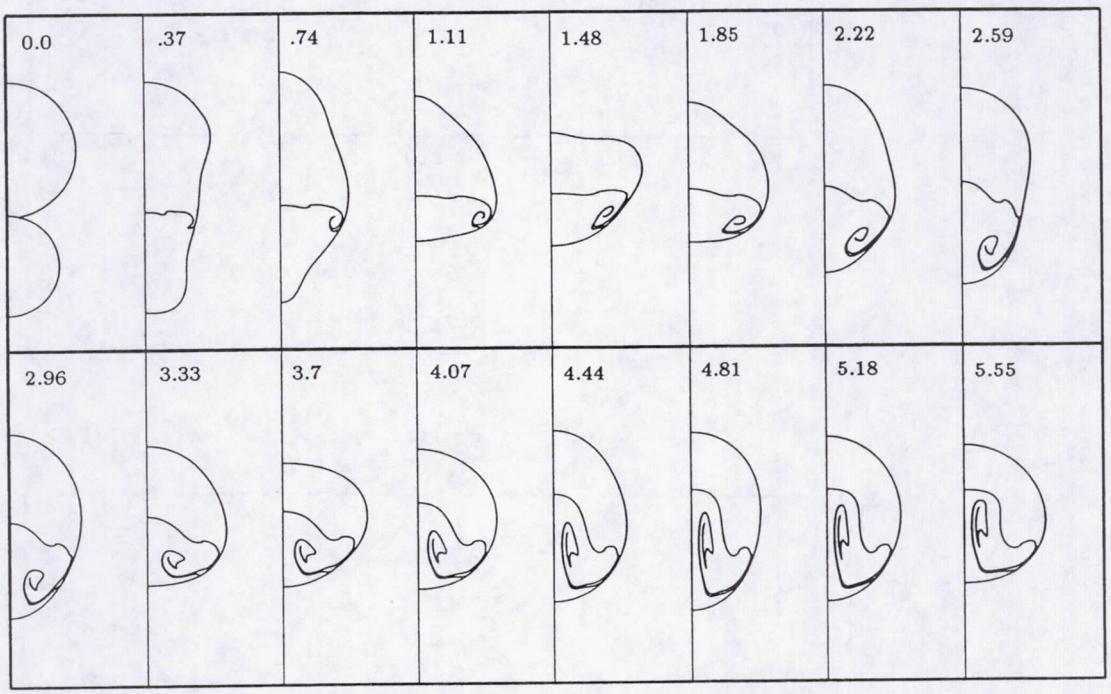

Figure 7. The evolution of two drops of unequal size following coalescence. Here, the viscosity of the drops is low, $Oh = 0.002$, and the fluid from the small drop is ejected across the large drop. $d_s/D = 0.667$, $\rho_d/\rho_o = 20.0$, and $\mu_d/\mu_o = 0.1$. Only part of the computational domain is shown.

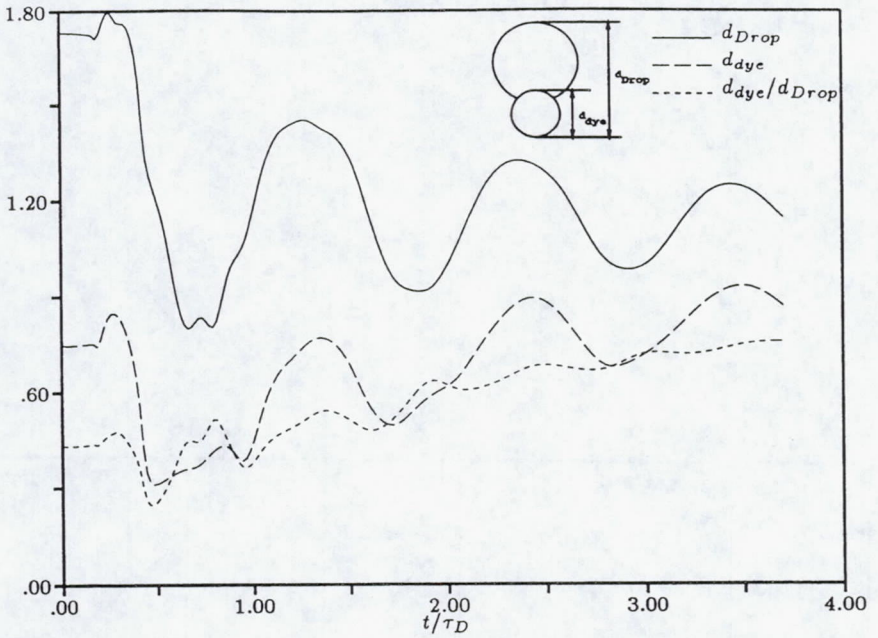

(a)

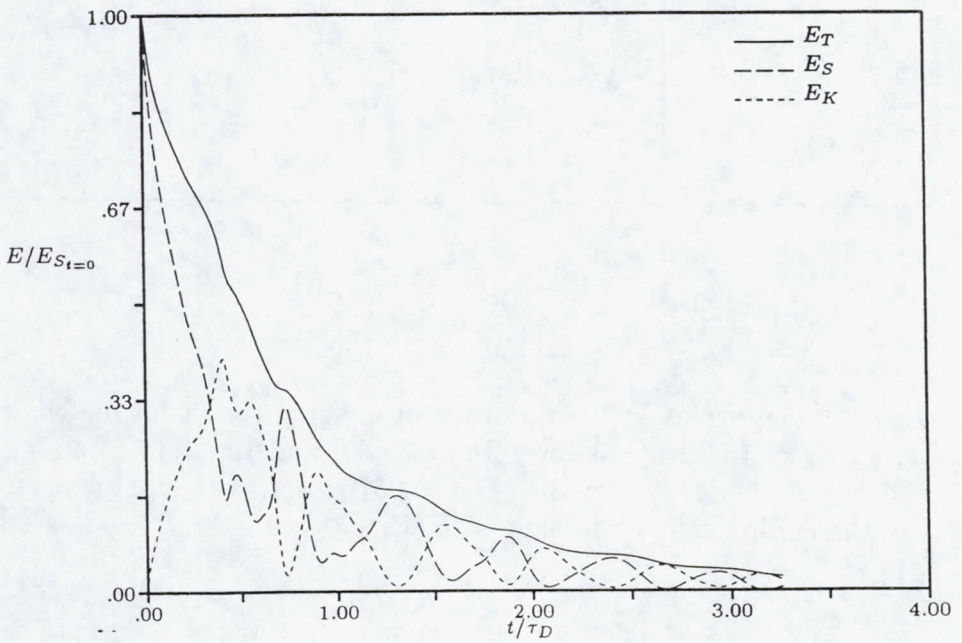

(b)

Figure 8. (a) Axial distance, penetration depth, and their ratio versus time for the drops in figure 7. (b) Non-dimensional kinetic, surface tension, and total energy based on initial surface tension energy versus time for the drops in figure 7.

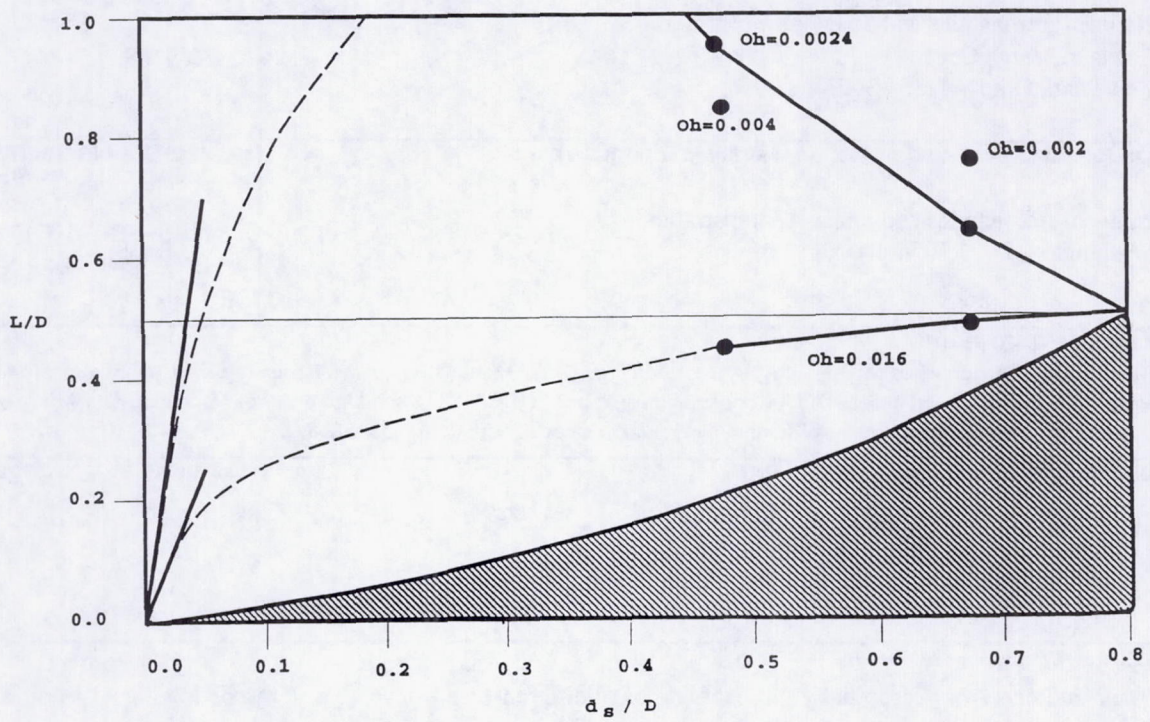

Figure 9. Penetration depth versus the ratio of the small drop diameter to the diameter of the combined drop for several values of Oh. The penetration depth can not be inside the cross-hatched region. The solid circles connected by solid lines are obtained by the numerical simulations, and the solid lines near the origin are experimental results for a drop coalescing with a flat interface. The dash lines are interpolations based on the numerical and experimental results for two Oh.

REPORT DOCUMENTATION PAGE

Form Approved
OMB No. 0704-0188

1. AGENCY USE ONLY (*Leave blank*)	2. REPORT DATE	3. REPORT TYPE AND DATES COVERED
	October 1994	Technical Memorandum

4. TITLE AND SUBTITLE

The Flow Induced by the Coalescence of Two Initially Stationary Drops

5. FUNDING NUMBERS

WU-505-90-5K

6. AUTHOR(S)

M.R. Nobari and G. Tryggvason

7. PERFORMING ORGANIZATION NAME(S) AND ADDRESS(ES)

National Aeronautics and Space Administration
Lewis Research Center
Cleveland, Ohio 44135-3191

8. PERFORMING ORGANIZATION REPORT NUMBER

E-9168

9. SPONSORING/MONITORING AGENCY NAME(S) AND ADDRESS(ES)

National Aeronautics and Space Administration
Washington, D.C. 20546-0001

10. SPONSORING/MONITORING AGENCY REPORT NUMBER

NASA TM-106752
ICOMP-94-24

11. SUPPLEMENTARY NOTES

M.R. Nobari, University of Michigan, Ann Arbor, Michigan 48823; and G. Tryggvason, Institute for Computational Mechanics in Propulsion (work funded under NASA Cooperative Agreement NCC3-233), and University of Michigan, Ann Arbor, Michigan 48823. ICOMP Program Director, Louis A. Povinelli, organization code 2600, (216) 433-5818.

12a. DISTRIBUTION/AVAILABILITY STATEMENT

Unclassified - Unlimited
Subject Category 34

12b. DISTRIBUTION CODE

13. ABSTRACT (*Maximum 200 words*)

The coalescence of two, initially stationary drops of different size is investigated by solving the unsteady, axisymmetric Navier-Stokes equations numerically, using a Front-Tracking/Finite Difference method. Initially, the drops are put next to each other and the film between them ruptured. Due to surface tension forces, the drops coalesce rapidly and the fluid from the small drop is injected into the larger one. For low nondimensional viscosity, or Ohnesorge number, little mixing takes place and the small drop fluid forms a blob near the point where the drops touched initially. For low Ohnesorge number, on the other hand, the small drop forms a jet that penetrates far into the large drop. The penetration depth also depends on the size ratio of the drops and we show that for a given fluid of sufficiently low viscosity, there is a maximum penetration depth for intermediate size ratios.

14. SUBJECT TERMS

Unsteady Navier-Stokes equations; Front-tracking method; Mixing due to coalescence

15. NUMBER OF PAGES
27

16. PRICE CODE
A03

17. SECURITY CLASSIFICATION OF REPORT	18. SECURITY CLASSIFICATION OF THIS PAGE	19. SECURITY CLASSIFICATION OF ABSTRACT	20. LIMITATION OF ABSTRACT
Unclassified	Unclassified	Unclassified	